Advanced Optimal Control Design for a Buck-Boost Converter in Photovoltaic Systems

Daniel-Marian BĂNCILĂ*, Ștefania-Cristiana COLBU, Dumitru POPESCU

Department of Automatic Control and Systems Engineering, Faculty of Automatic Control and Computers, National University of Science and Technology Politehnica Bucharest,
313 Splaiul Independenței, 060042, Bucharest, Romania
daniel.bancila@stud.acs.upb.ro (**Corresponding author*), stefania.colbu@stud.acs.upb.ro,
dumitru.popescu@upb.ro

Abstract: In the field of photovoltaic systems, the focus remains on the problem of increasing the energy conversion efficiency by reaching the maximum power output and optimizing the overall system performance while trying to reduce losses and costs in order to obtain a reliable and sustainable source of renewable energy. This paper proposes a control strategy for a DC-DC buck-boost converter integrated into a photovoltaic plant, utilizing an Advanced Linear Quadratic Regulator (LQR) approach enhanced with integral action. The proposed regulator is aimed to optimise the converter's performance and to ensure its stable operation under the influence of varying environmental conditions. The main challenge addressed by this paper is to keep the output voltage at a required setpoint, independent of the input voltage variations and/or the system dynamics. With an improved transient response and an incorporated integral action, the proposed regulator is confirmed to be effective in ensuring Maximum Power Point Tracking (MPPT) in a photovoltaic system. The results of the simulations reflect the efficiency of the recommended LQR-based control approach in achieving an optimal voltage regulation by providing a reliable and efficient solution for converters integrated into solar tracking systems.

Keywords: DC-DC buck-boost converter, Integral action, Optimal control, Photovoltaic system, Voltage regulation.

1. Introduction

The exploitation of renewable energy sources contributed to technological development and to many discoveries in the last 50 years and now it is feasible even at low costs to substitute the dependency on fossil fuels which implies greenhouse gas emissions. The path to a greener feature implied a lot of effort from the researchers in the last decades. It got them to the point where the most cost-effective, developed and tested with positive results are the solar and wind exploitation systems (Breyer et al., 2022). This paper is focused on the solar source, involving photovoltaic panels (PV) with a variable orientation.

Because the energy production from solar irradiance is inconsistent, a storage system is frequently needed (Iovine et al., 2017). Also, there are cases when the end customer needs a high amount of energy and DC/AC microgrid systems are used even to encapsulate more energy sources (Guerrero et al., 2013).

The challenges of improving the solar panels efficacy have also gone into exploring different ways of mounting the panels. Whilst one may think that only the panels on the ground, on top of buildings or on water surfaces were taken into account, many other ideas have been explored including adjustable panel angles and bioinspired solutions. For instance, Mihai, Olteanu & Popescu (2024) introduced a trajectory optimization method for panels with 2 degrees of freedom designed to optimize the output energy by maximizing the total amount of accessible solar irradiance. The topic of bioinspiration came into mind because the evolution of biodiversity led the micro-organisms to adapt in order to survive. This evolution has proved to develop many effective structures even when it comes to capturing the solar rays, needed by the plants for photosynthesis (Huang, Xu & Markides, 2023). In the same direction, the cooling system for PV panels can be implemented as inspired by the marine mussels (Lv et al., 2021).

Variations in irradiance and weather induce fluctuations in the power-voltage and current-voltage characteristics of a PV system. Consequently, different MPPT methodologies were introduced. Three general categories can be used to characterise MPPT techniques:

1. conventional methods, including approaches such as perturb and observe, hill climbing, and incremental conductance (Mao et al., 2020);

2. artificial intelligence algorithms, which employ optimization methods including genetic algorithms, artificial bee colony, particle swarm optimization, or artificial neural networks (ANN) (Mazumdar et al., 2024; Mao et al., 2020, Dučić et al., 2023);

3. advanced control strategies, which utilize model-based control approaches, including

https://doi.org/10.24846/v34i2y202501

both linear and nonlinear control approaches, such as sliding mode control (SMC), model predictive control (MPC), or fuzzy logic controllers (FLC) (Mazumdar et al., 2024).

Among the above-mentioned methods, advanced control strategies gained high interest in recent years because they promise to achieve an improved tracking efficiency along with stability. One such method is the LQR approach, applied in many control applications. LQR-based MPPT techniques have shown promising results, especially in the presence of parametric variations and disturbances.

Furthermore, the DC-DC converter was introduced in the literature to control the voltage received from the PV system. This is needed to ensure a stable voltage level, optional for the maximum extracted power for the battery or inverter which is connected. In order to do this, the voltage can be set up (boost) or down (buck). While the boost converter's efficiency has a direct correlation with the input voltage value, the buck converter's efficiency is inversely proportional to the input voltage (Ren et al., 2008). To combine both of them, the buck-boost converter was introduced, which is capable of increasing as well as decreasing the voltage, making it suitable for applications where the voltage from the PV panel has significant fluctuations. This fact gives the buck-boost converter the capability of maintaining the MPP for a PV through different weather conditions.

This study introduces an advanced control strategy for achieving an optimum efficiency and robustness of photovoltaic energy conversion over a spectrum of environmental conditions. The paper proposes a LQR with integral action for controlling a DC-DC buck-boost converter in a PV system for stable voltage regulation around the maximum power point, which is independent of input voltage change due to changes in irradiance and temperature. The research answers the growing need for stable and adaptive MPPT solutions in renewable energy systems.

The remainder of this paper is as follows. Section 2 presents related works that describe control methods in buck-boost converters. Section 3 refers to the employed materials and methods and offers details related to the general theoretical framework, the system's model and dynamics, and the advanced optimal control design. Section 4 assesses the results obtained by the applied regulator. Finally, Section 5 concludes this paper with the key findings about the performance of the proposed LQR controller and outlines possible future research directions.

2. Related Works

Various papers have been focused on advanced control algorithms for regulating the DC-DC converters and particularly the buck-boost converters in PV systems to attain the MPPT.

Several related applications involved charging algorithms for electrical vehicle (EV) batteries supplied by energy from PV systems. Dobrea et al. (2023) have proposed a conventional PID controller in combination with a hybrid FLC-PID controller to regulate a Phase-Shifted Full-Bridge (PSDB) converter in the charging process for an EV battery. The study highlighted the potential of the hybrid controller in rejecting the disturbances and improving the response time to provide an efficient charging method. Mani et al. (2023) also presented an ANN optimized hybrid energy management system for photovoltaic powered EVs. This approach introduced a High Gain Interleaved Boost Converter controlled by an MPC to optimize power production, while another boost converter ensured voltage stability. This study showed the advantage of ANN with respect to conventional Proportional-Integral (PI) controllers and underlined the potential of data-driven approaches to increase control results.

For standalone PV plants, Restrepo et al. (2022) introduced a digital implementation of a versatile buck-boost DC-DC converter control system. The authors presented an enhanced MPC algorithm that merges three critical control loops, namely MPPT, fast input voltage regulation, and high-bandwidth current control, all executed via a single digital signal controller. The system operated effectively in nominal buck mode, as well as under partial shadow conditions, when the activation of the PV module's bypass diodes leads to a MPP associated voltage lower than the battery voltage, forcing the system`s operation in boost mode.

Quezada et al. (2021) attempted to apply a Linear Quadratic Gaussian (LQG) controller for performance optimization for the buck-boost converter in a PV application. The regulator was deployed with an additional Kalman filter for regulating the output voltage and rejecting the disturbances. The proposed methodology has been verified and it ensured that LQG is capable of handling Gaussian noise and of optimizing output voltage regulation for the PV, with an estimation error of the states (the output voltage and the inductor current) of 1.5%.

Furthermore, Fard & Aldeen (2016) presented a LQR design for a system that incorporated a PV panel and a battery bank connected at a DC bus. This article explicitly considered the interaction between the PV system and the battery, addressing the challenges of regulating DC bus voltage and maximizing power extraction under varying conditions. The LQR was designed using linear matrix inequalities (LMIs) to achieve the best performance without any prior knowledge and the simulation results validated the efficacy of the approach that enhanced transient performance and robustness against load variation, achieving maximally 0.2*s* for a 4.2*KW* load demand, 0.5*s* for 6.4*K*, 0.8*s* for 10*KW*, and maximally 1*s* for 8*KW*.

For a photovoltaic-powered converter, Șahin & Okumuș (2018) explored the PI, FLC and SMC approaches. The performance and stability of these controllers were analysed in simulations and experimental setups under different environmental conditions. The outcomes reveal that, while the SMC has a better response time and ripple effect management, the FLC features a better performance in reducing overshoot and output voltage ripple, hence proving its potential for future renewable energy applications.

Despite a substantial body of research, the control algorithms for converters are still challenging, and additional work should also be carried out with regard to the robustness of the deployed algorithms.

3. Methods

3.1. General Theoretical Framework

The global theoretical framework consists of a particular strategy for controlling a buck-boost converter that can be supplied by a solar tracking system to enhance the entire system's efficacy.

The initial step of this methodology involves proposing a mathematical model of the converter. The state representation for the converter will be based on the correlation between the input and the output voltage. This model is taken into account for analysing the behaviour of the considered system and serves as a base for designing the optimal control strategy.

At the second stage level, an optimal controller including an integrative component is synthesized to regulate and stabilize the voltage delivered by the solar tracking system. The controller designed based on LQR is meant to ensure that the plant will deliver the expected maximum voltage potential, optimizing its performance and efficiency.

3.2. DC-DC Buck-boost Converter – Models and Dynamics

As energy consumption has skyrocketed in the last decades, the demand for DC-DC converters has increased for a variety of applications, such as electronic devices, avionics, satellites, vehicles and energy systems. To increase the converter's effectiveness and adaptability while reducing manufacturing and operating costs, this field has undergone substantial research and development. The configurations have expanded from single input-single output to multi-input-multiple output configurations (Aravind et al., 2024).

A DC-DC converter is an electronic device placed in a system, that is responsible for converting the DC input voltage into a distinct DC output voltage. There are multiple configurations of converters, but as this paper studies its applicability in a photovoltaic system, a buck-boost converter was chosen, because it is suitable for delivering the desired output voltage to the final load (the consumer or battery system). Additionally, the efficiency of a buck-boost converter ranges from 85% to 95% (Abdel-Rahim et al., 2022), which is advantageous for a converter because it reduces heat losses at higher loads.

Buck-boost converters can either step the voltage up or down with respect to the configuration. To make this possible the converter consists of an inductor which stores the energy while a switch (a transistor such as MOSFET) is ON, and releases it while it is OFF, a diode to direct the current flow to the output and to prevent backflow into the circuit when the switch is OFF, and a capacitor to filter the output voltage for ripple effect reduction and stabilisation. The electrical schema is represented in Figure 1.

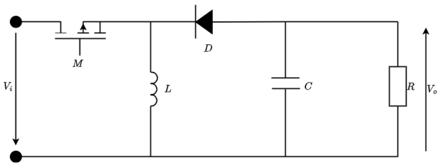

Figure 1. Buck-boost converter – circuit topology (Șahin & Okumuș, 2018)

The converter operates between the two states when the switch is ON and when it is OFF, as it is illustrated by the electrical equivalent circuits from Figure 2.

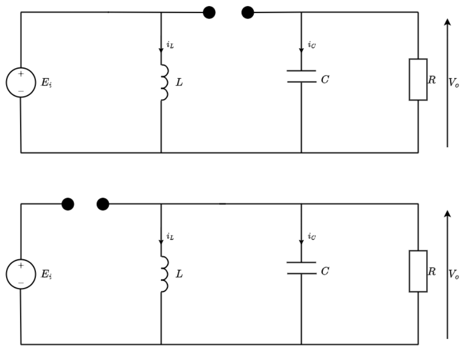

Figure 2. The equivalent circuits of the buck-boost converter: up - switch ON and down - switch OFF (Șahin & Okumuș, 2018)

One operating status is the continuous conduction mode (CCM), during which the inductor current never drops to zero, while the other known operating condition is discontinuous conduction mode (DCM), during which the current that passes through the inductor drops to zero.

The electrical parameters are the following: the voltage received from the photovoltaic panel, which is denoted in Figure 2 by the E_i source, alternatively denoted by V_i in Figure 1, the output voltage denoted by V_o, the inductance L in the circuit, the capacitance C, the output load resistance R, the frequency of switching between ON and OFF denoted by T_s in Figure 3, and the duty cycle D_c also in Figure 3 (the proportion of the ON-time in the overall switching period).

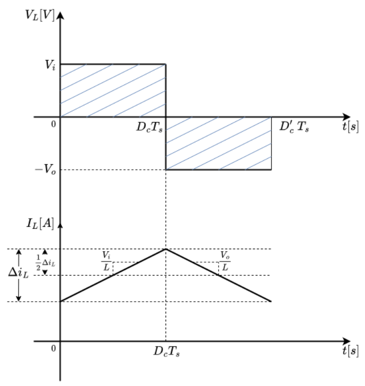

Figure 3. Variations of V_L and i_L with respect to the duty cycle and T_s

The ON state corresponds to the inductor voltage and is based on Kirchhoff's second law:

$$V_L = V_i \tag{1}$$

By applying Kirchhoff's second law, the OFF state can be expressed as:

$$V_L = -V_o \tag{2}$$

The voltage drop through the inductor is defined based on:

$$V_L(t) = L\frac{di_L}{dt} \tag{3}$$

ΔI_L denotes the inductor current ripple and is expressed as:

$$\Delta I_L = \frac{V_i D_c T_s}{L} \tag{4}$$

In Figure 3, $D_c^{'}$ is equal to $1 - D_c$ and when the voltage balance is established, the sum of the areas from the positive and negative parts of the graphic is equal to zero. Also, on steady state conditions the net switch over one switching cycle is zero (Sarikhani, Allahverdinejad & Hamzeh, 2020):

$$V_i D_c T_s - V_o D_c^{'} T_s = 0 \tag{5}$$

Consequently, the buck-boost converter's transfer function, consisting in the ratio between the output and the input voltage can be expressed as:

$$\frac{V_o}{V_i} = \frac{D_c}{1 - D_c} \tag{6}$$

The capacitor with the capacitance C has the voltage V_C and the current passing through it is denoted by i_C. When the switch is ON, the currents i_L and i_C are equal, so the voltage has the following value:

$$\frac{dV_C}{dt} = -\frac{i_L}{C} \tag{7}$$

When the switch is OFF, based on Kirchhoff's second law $V_L = -V_C$ and by applying Kirchhoff's first law, the previous relation becomes:

$$\frac{dV_C}{dt} = \frac{i_L - \frac{V_C}{R}}{C} \tag{8}$$

Taking into account i and V_C as state variables, using the duty cycle and the equations (3), (7) and (8) the state-space representation becomes (Sarikhani, Allahverdinejad & Hamzeh, 2020):

$$\begin{cases} \dfrac{di_L}{dt} = \dfrac{D_c V_i - (1 - D_c)V_C}{L} \\ \dfrac{dV_C}{dt} = \dfrac{(1 - D_c)i_L - \frac{V_C}{R}}{C} \end{cases} \tag{9}$$

The state vector is defined based on two primary states: the current passing through the inductor and the voltage across the capacitor – known as output voltage:

$$x = \begin{bmatrix} i_L \\ V_C \end{bmatrix} \tag{10}$$

Furthermore, the input vector is constructed using two key components, namely the input voltage and the duty cycle:

$$u = \begin{bmatrix} V_i \\ D_c \end{bmatrix} \tag{11}$$

The state-space equations can be represented as:

$$\begin{cases} \dot{x} = Ax + Bu \\ y = Cx + Du \end{cases} \tag{12}$$

with $A \in \mathbb{R}^{2x2}, B \in \mathbb{R}^{2x1}, C \in \mathbb{R}^{1x2}, D \in \mathbb{R}$ being the system's matrices.

3.3. Advanced LQR with Integral Action Design

The state-representation of the buck-boost converter is considered as:

$$\begin{cases} \dot{x} = Ax + Bu \\ x(t_0) = x_0 \end{cases} \tag{13}$$

with x being the state vector considered measurable for state feedback control. Additionally, (A,B) is assumed to be a stabilizable pair. In other words, there exists a K matrix that ensures the Hurwitz stability for the $(A-BK)$ matrix (Kirk, 2004).

A LQR strategy will be applied to attain both a tracking and regulation performance in the state-space representation. Implementing this regulator involves minimising the quadratic performance index L_c that penalizes the variations in the control input u and in the variation of the state vector x (Kirk, 2004). This implementation results in the formulation of a stabilizing state-feedback control law (Kirk, 2004):

$$L_c = \int_0^\infty \left[x^T Q x + u^T R u \right] dt \tag{14}$$

with the Q and R matrices being symmetric and positive definite. The optimal command is completed by the gain matrix K_L:

$$\begin{aligned} u &= -K_L x \\ K_L &= R^{-1} S B^T \end{aligned} \tag{15}$$

S is determined as the algebraic Riccati equation (Kirk, 2004) solution for LQR:

$$SA + A^T S - SBR^{-1} B^T S + Q = 0 \tag{16}$$

When considering that the purpose was to regulate a series of input voltages in order to attain the same stable voltage at the output, then it is necessary to introduce a reference $r(t)$ to be tracked. To assess the system performance, a tracking error is calculated by subtracting the output from the reference. Additionally, an integral control error is introduced:

$$x_e = \int e\, dt = \int (r - y)\, dt \tag{17}$$

Taking the first derivative of equation (17) and introducing in the output relations from equation (12), where u is considered to have no direct impact on the output, conducts to:

$$\begin{cases} \dot{x} = Ax + Bu \\ \dot{x}_e = r - Cx \end{cases} \tag{18}$$

In a matrix format it results that:

$$\begin{bmatrix} \dot{x} \\ \dot{x}_e \end{bmatrix} = \begin{bmatrix} A & 0 \\ -C & 0 \end{bmatrix} \begin{bmatrix} x \\ x_e \end{bmatrix} + \begin{bmatrix} B \\ 0 \end{bmatrix} u + \begin{bmatrix} 0 \\ I \end{bmatrix} r \tag{19}$$

By denoting the new extended state vector by $x_{ext}(t)$ it becomes:

$$\dot{x}_{ext} = A_{ext} x_{ext} + B_{ext} u + E_{ext} r \tag{20}$$

and by replacing the terms from equation (20) in equation (19), the extended matrices are defined:

$$\begin{gathered} x_{ext} = \begin{bmatrix} x \\ x_e \end{bmatrix},\ A_{ext} = \begin{bmatrix} A & 0 \\ -C & 0 \end{bmatrix},\ B_{ext} = \begin{bmatrix} B \\ 0 \end{bmatrix}, \\ C_{ext} = \begin{bmatrix} C & 0 \end{bmatrix}, \quad E_{ext} = \begin{bmatrix} 0 \\ I \end{bmatrix} \end{gathered} \tag{21}$$

This approach is known in the literature as LQR with integral action (Zarghoon et al., 2024), because the error is integrated as it was expressed in (17). The control law from equation (14) keeps the same form, but the expressed state is replaced by x_{ext} and the command takes the form:

$$u = -K_{L_{ext}} x_{ext} \tag{22}$$

where $K_{L_{ext}}$ is the extended control matrix that takes also into account the reference and is partitioned as:

$$K_{L_{ext}} = \left[K_L\, K_e \right] \tag{23}$$

By using it in equation (22) it can be seen that K_e controls the state $x_{ext}(t)$:

$$u = -\left[K_L\, K_e \right] \begin{bmatrix} x \\ x_e \end{bmatrix} = -K_L x - K_e x_e \tag{24}$$

From equation (17) results equation (25), which ca be expressed as:

$$u = -K_L x - K_e \int (r - y)dt \tag{25}$$

Equation (25) clearly shows that the integral control error is considered. Figure 4 illustrates the diagram of the system, including the regulator.

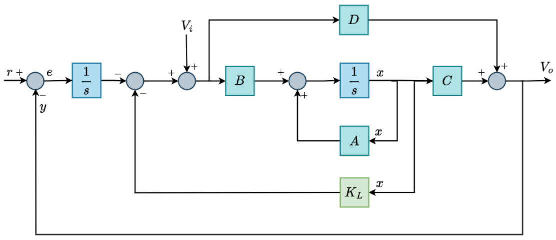

Figure 4. System block diagram including the controller

The input voltage is applied, as it can be observed in Figure 4, in the main control loop, for K_L to take action and before the matrices of the system.

4. Results and Discussion

In the current case study, the DC-DC converter was placed after a variable oriented photovoltaic panel which can generate in standard conditions up to $215W$ (Victron Energy, 2010). Consequently, the operational range of the converter is within $[0W, 215W]$, and, with regard to the voltage produced by the panel during the day, it is assumed that it usually has values in the interval $[12V, 37.4V]$, but it can be reduced during periods of partial shading. The desired converter's output voltage is $24V$ so that it can be stored in a battery or power a DC load.

The converter is analysed in CCM with ideal electrical components considered. Additionally, this will step up the input voltage if it is below $24V$ and will step it down if it is above $24V$. Taking into account the maximum voltage and power, the value of the maximum output current is $9A$. To ensure that the converter can handle this output current, the choice would be to slightly raise the output current for the converter at around $10A$.

The inductor of the converter should support a continuous current in conditions of maximum load. Also, the value of the inductance affects the voltage ripple and the stability of the converter. The capacitor serves to filter and effectively reduce the ripple in the voltage.

The considered photovoltaic panel SPM042152400 (Victron Energy, 2010) is capable of generating a maximum power of $215W$ at a voltage of $37.4V$ and a maximum current power of $5.75A$.

The converter's switching frequency is chosen to be $50kHz$, as it is a typical value for a converter in this class of applications. Also, in steady state the duty cycle from equation (6) can be expressed as:

$$D_c = \frac{V_o}{V_o + V_i} \simeq 0.4 \tag{26}$$

The efficiency of a converter under optimum conditions is around 95%, so the $215W$ power at the input will have the value of $204.25W$ at the output. Knowing that the target output voltage is $24V$, the output current is $8.51A$. Consequently, the resistance has the value of 2.8Ω.

Assuming that the value of the ripple current is 20% of that of the input current ($1.15A$), and taking into account equation (4), the value of the inductance is $0.254mH$.

Assuming a specified output voltage ripple of 1% ($\Delta V = 0.24V$), the capacitance can be computed as:

$$C = \frac{I_o D_c T_s}{\Delta V} \simeq 276.57\mu F \tag{27}$$

Accordingly, Table 1 presents the values of the parameters of the converter.

Table 1. Parameters of the buck-boost converter

Parameter	**Value**
Input Voltage V_i	$37.4V$
Output Voltage V_O	$24V$
Input Current I_i	$5.75A$
Output Current I_O	$8.51A$
Switching Frequency $1/T_s$	$50kHz$
Duty Cycle D_c	0.4
Inductance L	$0.254mH$
Capacitance C	$275.57\mu F$
Resistance R	2.8Ω

The state-space representation is defined by the following matrices:

$$A = \begin{bmatrix} -1291.32 & -3475.37 \\ 4096 & 0 \end{bmatrix} \qquad B = \begin{bmatrix} 64 \\ 0 \end{bmatrix} \tag{28}$$
$$C = \begin{bmatrix} 0 & 36.2 \end{bmatrix} \qquad D = \begin{bmatrix} 0 \end{bmatrix}$$

The open-loop simulation of the system for an input of $37.4V$ (the voltage delivered at the output of the SPM042152400 panel in MPP) results in the response from Figure 5.

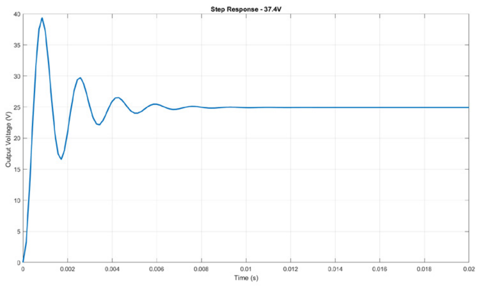

Figure 5. Open loop simulation of the system

The dynamic performance results from the simulation (Figure 5) are as follows: the rise time is 0.0003s, and the transient time reaches 0.006s. Also, the response is oscillatory until it settles at 24.9V with a maximum amplitude of 22.78V, the peak value is 39.36V, and the overshoot is 57.89%.

Given a reference voltage of 24V, the empirically chosen diagonal matrix Q is:

$$Q = \begin{bmatrix} 2100 & 0 \\ 0 & 233.8 \end{bmatrix} \tag{29}$$

The matrix R is chosen to be unitary to keep a balance between the performance of the system and the input, by not restricting the command of the system. Consequently, the gain matrix from equation (15) has the following computed value:

$$K_L = \begin{bmatrix} 42.61 & 11.21 \end{bmatrix} \tag{30}$$

The value of the voltage received from the photovoltaic panel is variable in different time intervals depending on the irradiance, temperature, and other environmental factors. Therefore, the controller is tested for different input voltages and it should keep at the output the desired voltage of 24V, required by the end user. When testing with different voltage values, the designed LQR keeps the stability of the output, but the output values differ, because the can be employed either for tracking or regulation, but not both at the same time. This situation leads to the final regulation solution for the converter, which consists in using an enhanced LQR with integral action that will have a reference to track and the input voltage is given additionally to the command signal as displayed in Figure 4.

The extended matrices describing the system in equation (21) for which the LQR with integral action is applied are:

$$A_{ext} = \begin{bmatrix} -1291.32 & -3475.37 & 0 \\ 4096 & 0 & 0 \\ 0 & -36.2 & 0 \end{bmatrix}; B_{ext} = \begin{bmatrix} 64 \\ 0 \\ 0 \end{bmatrix} \tag{31}$$
$$C_{ext} = \begin{bmatrix} 0 & 36.2 & 0 \end{bmatrix}; E_{ext} = \begin{bmatrix} 0 & 1 & 0 \end{bmatrix}^T$$

To calculate the control matrix K_{Lext}, K_e is considered to be unitary. It ensures that the integral error is directly involved in the control low and the cost function has no unwanted complexity added. In this context, the control matrix becomes:

$$K_{L_{\exp}} = \begin{bmatrix} 42.61 & 11.21 & 1 \end{bmatrix} \tag{32}$$

For simulating the entire system Matlab/Simulink R2021b was used, where the schema from Figure 4 was implemented with a 24V setpoint and the system output, for an initial step of 37.4$V$and a second step of 12V given at the time 0.4s, to simulate both the buck and boost modes of the converter. A comparative analysis of the open-loop (from Figure 6) and closed-loop (from Figure 7) responses indicates that the open-loop system is unable to regulate the output to the desired reference voltage, approximatively following the input signal. Additionally, the open-loop response in Figure 6, features transient oscillations before reaching a steady-state voltage level.

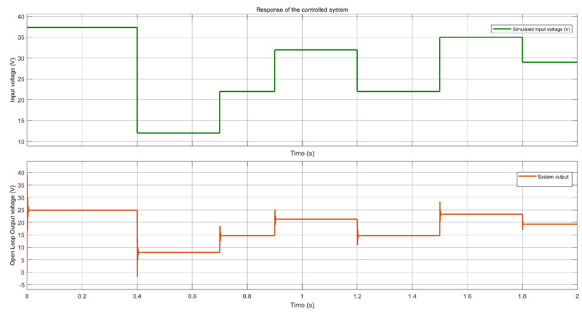

Figure 6. Response of the open-loop system, together with the simulated input voltage

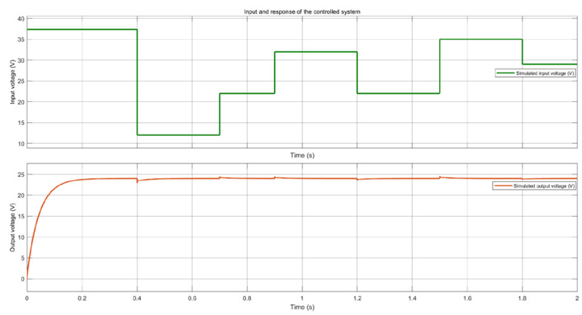

Figure 7. Response of the entire system with the LQR with an Integrative Component, together with the simulated input voltage

The dynamic performance results of the closed-loop system, from Figure 7, for the first given step with a reference voltage of $37.4V$ are as follows: the rise time is $0.0971s$, the settling time is $0.13s$, with zero overshoot and zero steady-state error.

The rise time and settling time are higher than the open loop, because the controller needs time to stabilize the oscillations of the system, but the time is still low and suitable for implementing the system. Also, the controlled system reaches the reference voltage and keeps it while the input voltage is first changed to $12V$ and even though there is a variation in the output which initially sets the voltage at $22.9V$ (still in the desired range of the converter`s operational capabilities), but with small oscillations, given by the RLC behaviour of the circuit, it stabilizes back to $24V$ in $0.21s$.

Several variations were introduced in the input of the controlled system. These values were chosen to emulate values that may be obtained in a real-world implementation of a photovoltaic panel. The input varies as follows: it is set at $37.4V$ to show how the system behaves at the maximum voltage associated with the MPP, the input is reduced to $12V$ to demonstrate the system`s capability to switch from the buck to the boost mode, it is set at $22V$, then at $32V$ to view the result of switching from the boost to the buck mode, then back to $22V$ to show that reverse switching is still possible, then at $35V$ to go back on the boost mode and in the end at $29V$ for demonstrating that even for this wide range of inputs the system can still go back to the desired $24V$ output in a time of around $0.2s$. Therefore, the robustness, stability and suitability of this converter with the introduced control solution for application in photovoltaic systems were proven.

To validate the performance of the proposed advanced LQR controller with integral action for buck-boost converters in PV systems, a comparative analysis was conducted in relation to the strategies presented in Section 2. In comparison with the hybrid FLC-PID of Dobrea et al. (2023), the proposed regulator guaranteed a zero steady-state error and no overshoot but with a similar disturbance rejection. In comparison with the ANN-based MPC of Mani et al. (2023), the proposed approach offers an analytical and computationally efficient solution with a robust control over wide input ranges. While Restrepo et al. (2022) introduced a MPC with multiple control loops performing effectively under partial shading conditions, the proposed controller matches its stability with a simpler design. To that, the integral action improves the tracking performance in comparison with the standard LQG of Quezada et al. (2021), as well as the setpoint accuracy compared with the LQR-LMI approach of Fard & Aldeen (2016). It performs better than PI, FLC, and SMC (Șahin & Okumuș, 2018) with regard to steady-state precision and overshoot elimination. Overall, the proposed controller provides an optimal trade-off between simplicity, reliability, and performance, making it a promising candidate for buck-boost regulation in renewable energy systems.

5. Conclusions

This study focused on a PV system's role in maintaining a constant output voltage in the presence of environmental changes and on improving the photovoltaic system's efficiency and energy output.

The converter connected to a $215W$ photovoltaic panel has a desired output of $24V$ and it was controlled in order to achieve this output with a wide range of voltages coming from the panel. Initially, the converter was modelled and from its mathematical equations resulted its state-space model. For this model a LQR was designed that minimizes the cost function. This controller was tested, which revealed that its limits are the sensitivity to disturbances and the reference tracking for various input voltages from zero to $37.4V$ (a voltage corresponding to MPP). Consequently, a LQR enhanced with integral action was added which makes up the novelty of this paper.

The proposed advanced LQR enhanced with integral action introduced the error as a new state and the system was redesigned to minimize the new integral criterion. This lead to zero steady-state error, an improved disturbance rejection by penalizing the accumulated error, and to actively compensating for disturbances in the input voltage, so it smoothened the tracking of dynamic input voltages coming in the specified interval from the panel. This controller was proved to have a robustness which makes it suitable for real-world application and also its general performance was in the desired range, as it rapidly arrived at the required output and reacted to input voltage changes with small oscillations, that did not cause issues to the system components.

In the schema depicting the advanced LQR enhanced with an integrative component, the input voltage was introduced in the main control loop, to be taken into account by the controller and it was added to the command signal, as an anticipative action to it, emphasising that the input was applied directly to the system.

Future directions would focus on testing the proposed controlled converter into a larger system designed for a renewable energy application. Such a system would consist of a photovoltaic panel, like the one for which the input range for the previous simulations was computed. Also, this panel would be connected to a motor used for tilting the panel, in order to maximize the solar energy production at each moment of the day. Furthermore, a robustness analysis would be carried out for the entire photovoltaic system, which will reveal the stability margins of a region suitable for keeping the system still stable, under parametric uncertainties, represented by changes in environmental conditions and by a slight degradation of the system over time.

Another future direction inspired by the artificial intelligence approaches from the literature (Mani et al., 2023) would be to enhance the capability of the LQR controller, by adding a data-driven controller before the already employed one to regulate it.

REFERENCES

Abdel-Rahim, O., Chub, A., Blinov, A. et al. (2022) An Efficient Non-Inverting Buck-Boost Converter with Improved Step Up/Down Ability. *Energies*. 15(13), art. no. 4550. https://doi.org/10.3390/ en15134550.

Aravind, R., Bharatiraja, C., Verma, R. et al. (2024) Multi-Port Non-Isolated DC-DC Converters and Their Control Techniques for the Applications of Renewable Energy. *IEEE Access*. 12, 88458 – 88491. https://doi.org/10.1109/ACCESS.2024.3413354.

Breyer, C., Khalili, S., Bogdanov, D. et al. (2022) On the History and Future of 100% Renewable Energy Systems Research. *IEEE Access*. 10, 78176-78218. https://doi.org/10.1109/ACCESS.2022.3193402.

Dobrea, M.A., Iliescu, S.-S., Arghira, N. et al. (2023) Modeling of a Hybrid Controller for Electric Vehicle Battery Charging Using Photovoltaic Panels. *Studies in Informatics and Control*. 32(4), 27-35. https://doi.org/10.24846/v32i4y202303.

Dučić, N., Dragićević, S., Stepanić, P. et al. (2023) Development of Hybrid Model based on Artificial Intelligence for Maximizing Solar Energy Yield. *Studies in Informatics and Control*. 32(4), 95-104. https://doi.org/10.24846/v32i4y202309.

Fard, M. & Aldeen, M. (2016) Linear Quadratic Regulator design for a hybrid photovoltaic-battery system. In: *2016 Australian Control Conference (AuCC), 3-4 November 2016, Newcastle, NSW, Australia*. Piscataway, NJ, USA, IEEE. pp. 347-352.

Guerrero, J. M., Loh, P. C., Lee, T.-L et al. (2013) Advanced Control Architectures for Intelligent Microgrids- Part II: Power Quality, Energy Storage, and AC/DC Microgrids. *IEEE Transactions on Industrial Electronics*. 60(4), 1263-1270. https://doi.org/10.1109/TIE.2012.2196889.

Huang, G., Xu, J. & Markides, C. N. (2023) High-efficiency bio-inspired hybrid multi-generation photovoltaic leaf. *Nature Communications*. 14(1), art. no. 3344. https://doi.org/10.1038/s41467-023-38984-7.

Iovine, A., Siad, S. B., Damm, G. et al. (2017) Nonlinear Control of a DC Microgrid for the Integration of Photovoltaic Panels. *IEEE Transactions on Automation Science and Engineering*. 14(2), 524-535. https://doi.org/10.1109/TASE.2017.2662742.

Kirk, D.E. (2004) *Optimal Control Theory: An Introduction*. Garden City, NY, USA, Dover Publications.

Lv, T., Sun, L., Yang, Y. et al. (2021) Bio-inspired hydrogel with all-weather adhesion, cooling and reusability functions for photovoltaic panels. *Solar Energy*. 216, 358-364. https://doi.org/10.1016/ j.solener.2021.01.028.

Mani, V., Yarlagadda, S.R., Ravipati, S. et al. (2023) ANN Optimized Hybrid Energy Management Control System for Electric Vehicles. *Studies in Informatics and Control*. 32(1), 101-110. https://doi.org/10.24846 /v32i1y202310.

Mao, M., Cui, L., Zhang, Q. et al. (2020) Classification and summarization of solar photovoltaic MPPT techniques: A review based on traditional and intelligent control strategies. *Energy Reports*. 6, 1312-1327. https://doi.org/10.1016/ j.egyr.2020.05.013.

Mazumdar, D., Sain, C., Biswas, P. K. et al. (2024) Overview of Solar Photovoltaic MPPT Methods: A State of the Art on Conventional and Artificial Intelligence Control Techniques. *International Transactions on Electrical Energy Systems*. 2024(1), art. no. 8363342. https://doi.org/10.1155/2024/ 8363342.

Mihai, L., Olteanu, S.C. & Popescu, D. (2024) Trajectory Optimisation for Photovoltaic Panels with 2 Degrees of Freedom. *Studies in Informatics and Control*. 33(4), 25-35. https://doi.org/10.24846/v33i4y202403.

Quezada, D., Beltran, C., Rohten, J. et al. (2021) Linear Quadratic Control design for a Buck-Boost Power Converter supplied by a Solar array. In: *2021 IEEE International Conference on Automation/XXIV Congress of the Chilean Association of Automatic Control (ICA-ACCA)*, *22-26 March 2021, Valparaiso, Chile*. Piscataway, NJ, USA, IEEE. pp. 1-6.

Ren, X., Ruan, X., Qian, H. et al. (2008) Three-Mode Dual-Frequency Two-Edge Modulation Scheme for Four-Switch Buck–Boost Converter. *IEEE Transactions on Power Electronics*. 24(2), 499-509. https://doi.org/10.1109/TPEL.2008.2005578.

Restrepo, C., Barrueto, B., Murillo-Yarce, D. et al. (2022) Improved Model Predictive Current Control of the Versatile Buck-Boost Converter for a Photovoltaic Application. *IEEE Transactions on Energy Conversion.* 37(3), 1505-1519. https://doi.org/10.1109/TEC.2022.3183986.

shani, A., Allahverdinejad, B. & Hamzeh, M. (2020) A Nonisolated Buck–Boost DC–DC Converter with Continuous Input Current for Photovoltaic Applications. *IEEE Journal of Emerging and Selected Topics in Power Electronics*. 9(1), 804-811. https://doi.org/10.1109/JESTPE.2020.2985844.

Șahin, M. E. & Okumuș, H.I. (2018) Comparison of Different Controllers and Stability Analysis for Photovoltaic Powered Buck-Boost DC-DC Converter. *Electric Power Components and Systems*. 46(2), 149–161. https://doi.org/10.1080/15325008.2018.1436617.

Victron Energy. (2010) *BlueSolar Monocrystalline Panels*. https://www.victronenergy.com/upload/documents/Datasheet-BlueSolar-Monocrystalline-Panels-EN-.pdf [Accessed 5th January 2025].

Zarghoon, S., Emebu, S., Matušů, R, et al. (2024) Full-state feedback LQR with integral gain for control of induction heating of steel billet. *Engineering Science and Technology, an International Journal*. 55, art. no. 101721. https://doi.org/10.1016/j.jestch.2024.101721.